

ORIGINAL RESEARCH

Open Access



From bench to bedside: $^{64}\text{Cu}/^{177}\text{Lu}$ 1C1m-Fc anti TEM-1: mice-to-human dosimetry extrapolations for future theranostic applications

Silvano Gnesin¹ , Nicolas Chouin² , Michel Chere³ , Steven Mark Dunn⁴ , Niklaus Schaefer⁵ , Alain Faivre-Chauvet³ , John O. Prior^{5*} and Judith Anna Delage⁶

Abstract

The development of diagnostic and therapeutic radiopharmaceuticals is an hot topic in nuclear medicine. Several radiolabeled antibodies are under development necessitating both biokinetic and dosimetry extrapolations for effective human translation. The validation of different animal-to-human dosimetry extrapolation methods still is an open issue. This study reports the mice-to-human dosimetry extrapolation of $^{64}\text{Cu}/^{177}\text{Lu}$ 1C1m-Fc anti-TEM-1 for theranostic application in soft-tissue sarcomas. We adopt four methods; direct mice-to-human extrapolation (M1); dosimetry extrapolation considering a relative mass scaling factor (M2), application of a metabolic scaling factor (M3) and combination of M2 and M3 (M4). Predicted in-human dosimetry for the ^{64}Cu]Cu-1C1m-Fc resulted in an effective dose of 0.05 mSv/MBq. Absorbed dose (AD) extrapolation for the ^{177}Lu]Lu-1C1m-Fc indicated that the AD of 2 Gy and 4 Gy to the red-marrow and total-body can be reached with 5–10 GBq and 25–30 GBq of therapeutic activity administration respectively depending on applied dosimetry method. Dosimetry extrapolation methods provided significantly different absorbed doses in organs. Dosimetry properties for the ^{64}Cu]Cu-1C1m-Fc are suitable for a diagnostic in-human use. The therapeutic application of ^{177}Lu]Lu-1C1m-Fc presents challenges and would benefit from further assessments in animals' models such as dogs before moving into the clinic.

Keywords Theranostic, Fusion protein antibody, Tumor endothelial marker 1, Copper-64, Lutetium-177, PET imaging, Radioimmunotherapy, Dosimetry, Dose extrapolation, Clinical translation

*Correspondence:

John O. Prior
John.Prior@chuv.ch

¹ Institute of Radiation Physics, Lausanne University Hospital and University of Lausanne, 1011 Lausanne, Switzerland

² Inserm, CNRS, University of Angers, Oniris, CRCI2NA, University of Nantes, Nantes, France

³ CHU Nantes, CNRS, Inserm, CRCINA, University of Nantes, 44000 Nantes, France

⁴ LabCore, Ludwig Institute for Cancer Research, Lausanne University Hospital and University of Lausanne, 1066 Epalinges, Switzerland

⁵ Department of Nuclear Medicine and Molecular Imaging, Lausanne University Hospital and University of Lausanne, Rue du Bugnon 46, 1011 Lausanne, Switzerland

⁶ Radiopharmacy Unit, Department of Pharmacy, Lausanne University Hospital and University of Lausanne, 1011 Lausanne, Switzerland

Introduction

TEM-1, also named endosialin or CD248, is a transmembrane cell surface glycoprotein expressed on pericytes and fibroblasts during tissue development, tumor neo-vascularization and inflammation [1]. In normal adults, TEM-1 protein expression appears to be limited to normal endometrial stroma and occasional fibroblasts [1, 2]. In pathological indications, the presence of TEM-1 has been reported in a wide variety of cell types associated with malignant diseases [3] and clinical studies have shown a direct correlation between TEM-1 transcript levels and patients outcomes with elevated levels of TEM-1 associated with nodal involvement and disease

progression [4, 5]. Based on its pattern of expression and its association with pathology, TEM-1 is considered by the research community as a promising target [6, 7].

In humans, it has been recently reported that soft tissue sarcomas (STS) express TEM-1 with a high level of staining (96% of expression) [8]. Sarcoma appears as an attractive target as TEM-1 is simultaneously expressed in the TEM-1 vasculature, stroma and tumor cells [9]. Currently, the medical care for STS comprises surgery for local disease, radiotherapy and chemotherapy, but the prognosis of patients with metastasis or unresectable tumor is poor, with an overall survival of less than 50% at 5 years for advanced stages [10]. The development of new therapeutic strategies with new classes of molecules is thus needed.

Radiotheranostics is a rapidly-evolving branch of theranostics, with emerging opportunities for the personalization of therapy, facilitating potential improvements in patient care and clinical outcome. Nowadays, radiotheranostics is at a tipping point, and is moving into the mainstream of cancer therapeutics [11]. Theranostics radiopharmaceuticals carry alpha or beta emitters to the target tissues by attaching ligands such as small molecules, peptides or antibodies, to chelators that complex radioisotopes for systemic delivery.

We previously developed and tested preclinically a fully human single-chain variable fragment (scFv)-Fc fusion, 1C1m-Fc, cross-reacting with both murine and human TEM-1. This fusion protein antibody was conjugated with DOTA and radiolabeled with ^{64}Cu for PET imaging [12] and with ^{177}Lu for therapeutic purposes [13, 14]. The antibody biodistribution and imaging contrast were improved and our radiolabeled fusion protein antibody was validated as a potential theranostic tool to target TEM-1 with high quality PET/CT images and promising therapeutic applications.

Small animal data are essential to obtain successful clinical translation of new radiopharmaceuticals. Similarly, response and toxicity prediction are key steps for the implementation of a new theranostic agent. In contrast to chemotherapy or biologic treatments, the radiation delivery and the biological response to radiation can be modeled mathematically and used to understand the parameters of the treatment that are most important in influencing efficacy and toxicity [15]. The absorbed dose (AD), defined as the energy absorbed per unit of mass of tissue, mediated the biological effects of radionuclide therapy may be used to predict biological response [16]. In a preclinical study, the assessment of the AD to target tissues, based on biokinetic data, is usually obtained from the measurement of the *ex-vivo* activity present in dissected source organs performed at multiple time points

after the injection of the radiopharmaceutical in a cohort of a specific animal model.

In view of a future transfer of our preclinical results obtained in mice with the tested radiolabeled fusion protein antibody to a first-in-human clinical study for STS disease, it is mandatory to perform the animal-to-human radiation dosimetry translation by extrapolating the observed murine data to the human model [17, 18]. Due to the difference in size organ masses in relation to the whole-body weight, and metabolic rates across the animal species (mice and the human in this case), reference dosimetry extrapolation methods have been developed [17, 19]. Unfortunately, the reliability and validation of these different extrapolation approaches are rarely documented in the published literature [18]. Hence, animal to human dosimetry extrapolation remains a matter of further study and development.

The aim of this study is to present and discuss the first extrapolation of AD to humans from previously obtained mice data to support the possible theranostic application of the TEM-1 compound. We applied reference computational methods of animal-to-human AD extrapolation as recently reported by Ciccone et al. [19].

Materials and methods

Radiopharmaceutical

A single-chain variable fragment (scFv)-Fc fusion, named 1C1m-Fc (Molecular Weight = 106,196.8 Da), synthesized at the LABCore immunoglobulin discovery and engineering facility, Ludwig Institute for Cancer Research Lausanne, was used. This fusion protein antibody has the properties to bind to the extracellular domain of both human and murine TEM-1 antigen and has been described previously [13, 20].

The conjugation and radiolabeling method as well as the different steps of the preclinical evaluation of the 1C1m-Fc fusion protein antibody, radiolabeled either with ^{64}Cu (half-life of 12.7 h) or ^{177}Lu (half-life of 6.6 days) was described earlier in Delage et al. [12–14].

Biodistribution study

Murine xenograft model was described in Delage et al. [13]. Biodistribution studies were performed in female Balb/c nude mice (Charles River Laboratories, Wilmington, MA, USA) aged from 6 to 10 weeks. Methodology of the biodistribution studies was described in our previous articles [12–14].

The biodistribution data, based on *ex-vivo* source organ measurements in a calibrated gamma counter, obtained with [^{177}Lu]Lu-1C1m-Fc conjugated with 1 and 3 DOTA at 4, 24, 48, 72 h and 6 days ($n=3$ per timepoint) [13, 14] and with [^{64}Cu]Cu-1C1m-Fc conjugated with 3 DOTA at

4 h ($n=4$), 24 h ($n=5$) and 48 h ($n=5$) [12] were used for the dosimetry extrapolation.

Dosimetry

We computed the time-integrated activity coefficients (TIACs) for the three radiolabeled compounds by time integration of normalized time activity curves (nTAC) as reported in [12–14]. Source organ TIACs, corrected for tumor sink effects [21], were computed for the average nTACs and the nTACs obtained by fitting the average time activity data \pm 1SD, hence providing an upper/lower TIAC values defining the range of variability of each source organ TIAC for each radiolabeled compound.

We obtained mice-to-human TIAC extrapolations according to four methods as described and applied in previous literature [19, 22].

Method 1 (M1) considered a direct TIAC extrapolation from mice (TIAC_m) to human (TIAC_h).

$$\text{TIAC}_{h,M1}(\text{organ}) = \text{TIAC}_m(\text{organ}) \quad (1)$$

Method 2 (M2) applied a corrective scaling factor to the mice organ source organ TIAC to consider the relative mass ratios between the considered source organ masses ($m(\text{organ})$) and the whole-body masses (WB) in mice and humans.

$$\text{TIAC}_{h,M2}(\text{organ}) = \text{TIAC}_m(\text{organ}) \times \left(\frac{m(\text{organ})_h/\text{WB}_h}{m(\text{organ})_m/\text{WB}_m} \right) \quad (2)$$

In Method 3 (M3), the human source organ TIACs were obtained by mono-exponential time integration of murine nTAC where the organ specific biological half-life (\square_b) was scaled to consider the different metabolic rate between species.

$$\text{TIAC}_{h,M3}(\text{organ}) = \frac{C_{m,\text{organ}}(t=0)}{k_b^{-1} \times \lambda_b + \lambda_p} \quad (3)$$

More detail about the application of this method can be found in previous publications [19, 23].

Method 4 (M4) combined the relative mass scaling applied in M2 and the metabolic scaling used in M3.

$$\text{TIAC}_{h,M4}(\text{organ}) = \text{TIAC}_{h,M3}(\text{organ}) \times \left(\frac{m(\text{organ})_h/\text{WB}_h}{m(\text{organ})_m/\text{WB}_m} \right) \quad (4)$$

Relative mass scaling applied in M2 and M4 considered source organ masses in murine models as reported in previous literature [12–14] and the source organ human masses of the adult male and female ICRP-89 models [24].

For the three considered radiolabeled compounds, extrapolated human source organ TIAC (average, upper

and lower values) were used as input for the kinetic model in the OLINDA/EXM 2.1 software (HERMES Medical Solution AB, Stockholm, Sweden) [25]. The software computed the target organ absorbed doses (average, upper and lower AD) and effective doses (E) for the male, female and the gender averaged adult human subjects using the formalism indicated in the ICRP-103 publication [26].

To obtain predictions of the amount of activity to administer in human patients in view of a possible therapeutic translation of the ¹⁷⁷Lu radiolabeled compounds, we computed the maximum tolerable cumulated activity compatible with the levels of toxicity in possible limiting organs such as the heart wall, the kidneys, the liver, the lungs, the red-marrow, and the uterus. We considered AD toxicity thresholds from data available for radiopharmaceutical therapy for nuclear medicine procedures. In case of missing data, toxicity thresholds accepted for external beam irradiation therapy (EBRT) were used instead. Reference safety AD limits for thoracic organs such as the heart wall (30 Gy) and the lungs (20 Gy) were from Kong et al. [27]. The 40 Gy considered for a total liver irradiation comes from the toxicity level adopted in ⁹⁰Y selective internal radiation therapy [28]. In this work we assumed a maximum tolerable AD of 30 Gy to the kidneys, which is commonly used in therapeutic applications of ¹⁷⁷Lu by radiologists, even if a clear dose/safety threshold has not been yet established and reasonable toxicity limits are beyond this assumed AD level [29]. The safety limits of 16 Gy to the uterus was derived from EBRT and considers the possibility to maintain the fertility in young female patients [30]. Lastly the 2 Gy and 4 Gy safety limits for the red-marrow and the whole body are adopted from the ¹³¹I [31] and [¹³¹I]-I-MIBG [32] therapy respectively. The AD threshold of 60 Gy to obtain tumor control in STS was taken from EBRT [33]. In particular, to compute the activity required to reach the target tumor dose, we considered the tumor to normal liver AD ratio of 1.4 obtained for the [¹⁷⁷Lu]Lu-1C1m-Fc 1 DOTA configuration [14]. This calculation applies only to M1 for which the 1.4 tumor-to-liver ratio was computed.

For sake of comparison, we compared target organ AD obtained for the diagnostic [⁶⁴Cu]Cu-1C1m-Fc with two other diagnostic radiolabeled antibodies already tested in human, the [⁶⁴Cu]Cu-DOTA-Trastuzumab [34] and the [⁸⁹Zr]Zr-cmAb U36 [35] respectively.

Results

For the four dosimetry methods described above (M1–M4), we reported the average values of source organ TIACs extrapolated to the human from previously published mice data for the [¹⁷⁷Lu]Lu-1C1m-Fc conjugated to 1 DOTA (Table 1), and 3 DOTA (Table 2) and the

Table 1 Mice-to-human extrapolated dosimetry for [¹⁷⁷Lu]Lu-1C1m-Fc 1 DOTA

[¹⁷⁷ Lu]Lu-1C1m-Fc 1 DOTA	TIAC (MBq.h/MBq)							
	M1		M2		M3		M4	
	M	F	M	F	M	F	M	F
Left colon	0.708	0.697	0.154	0.188	1.134	1.118	0.247	0.301
Small intestine	3.548	3.548	0.747	0.800	5.499	5.499	1.158	1.240
Stomach cont	0.824	0.824	0.324	0.365	0.824	0.824	0.324	0.365
Right colon	0.944	0.945	0.205	0.254	1.513	1.515	0.329	0.407
Rectum	0.456	0.465	0.099	0.125	0.731	0.745	0.159	0.200
Heart cont	1.961	1.961	2.436	2.150	5.364	5.364	3.455	3.050
Heart wall	0.509	0.509	0.402	0.371	1.066	1.066	0.843	0.777
Kidneys	3.592	3.592	0.919	0.992	4.928	4.928	1.261	1.361
Liver	22.894	22.894	9.183	8.690	22.401	22.401	8.985	8.503
Lungs	1.101	1.101	2.166	2.087	2.507	2.507	4.931	4.749
Ovaries		0.468		0.036		0.598		0.049
Salivary glands	0.800	0.852	0.161	0.161	0.800	0.852	0.161	0.172
Red marrow	2.211	2.475	5.588	5.230	2.922	3.070	7.386	6.912
Spleen	1.132	1.132	0.454	0.478	1.476	1.476	0.591	0.623
UB	0.186	0.199	0.677	0.624	0.186	0.199	0.677	0.665
Uterus		2.886		0.620		2.886		0.661
Total body	111.1	111.1	111.1	111.1	111.1	111.1	111.1	111.1
Rest of body	70.2	66.5	87.6	87.9	59.7	56.0	80.6	81.0

[¹⁷⁷Lu]Lu-1C1m-Fc 1 DOTA mice-to-human extrapolation of average source organ TIACs was obtained with the four considered dosimetry methods (M1-M4) for both the adult male (M) and female (F) human subjects

Table 2 Mice-to-human extrapolated dosimetry for [¹⁷⁷Lu]Lu-1C1m-Fc 3 DOTA

[¹⁷⁷ Lu]Lu-1C1m-Fc 3 DOTA	TIAC (MBq.h/MBq)							
	M1		M2		M3		M4	
	M	F	M	F	M	F	M	F
Left colon	0.609	0.600	0.130	0.158	0.985	0.970	0.210	0.255
Small intestine	2.842	2.842	0.570	0.755	4.521	4.521	0.906	0.970
Stomach cont	0.575	0.575	0.636	0.716	0.553	0.570	0.612	0.710
Right colon	0.651	0.687	0.139	0.181	1.313	1.315	0.280	0.346
Rectum	0.113	0.141	0.201	0.223	0.635	0.647	0.135	0.170
Heart cont	1.083	1.083	0.764	0.835	2.841	2.815	2.003	1.752
Heart wall	0.343	0.343	0.157	0.179	0.891	0.891	0.407	0.375
Kidneys	2.129	2.129	0.553	0.597	4.226	4.226	1.098	1.185
Liver	31.678	31.678	12.321	11.659	31.678	31.678	12.321	11.659
Lungs	0.744	0.744	1.646	1.964	1.894	1.894	4.191	4.037
Ovaries		0.241		0.013		0.448		0.024
Red marrow	2.508	2.635	2.508	2.635	6.517	6.847	6.517	6.847
Spleen	1.163	1.163	0.536	0.565	1.163	1.163	0.536	0.565
UB	0.140	0.140	0.140	0.140	0.140	0.140	0.140	0.140
Uterus		1.727		0.581		0.581		0.581
Total body	98.8	98.8	98.8	98.8	98.8	98.8	98.8	98.8
Rest of body	54.2	52.1	78.5	77.6	41.4	40.1	69.4	69.2

[¹⁷⁷Lu]Lu-1C1m-Fc 3 DOTA mice-to-human extrapolation of average source organ TIACs was obtained with the four considered dosimetry methods (M1-M4) for both the adult male (M) and female (F) human subjects

[⁶⁴Cu]Cu-1C1m-Fc conjugated with 3 DOTA (Table 3). Full TIAC data including the inf/sup values are provided in the Additional file 1: Tables S1, S2 and S3.

In Table 4 we report the Olinda generated target organ AD for the gender average adult human subject for the main irradiated organs for the ¹⁷⁷Lu radiolabeled compound using the four extrapolation methods described above (M1-M4).

Table 5 reports the averaged AD for the [⁶⁴Cu]Cu-1C1m-Fc 3 DOTA and for sake of comparison AD from the [⁶⁴Cu]Cu-DOTA-Trastuzumab [34] and the [⁸⁹Zr]Zr-cmAb U36 [35] respectively.

In Figs. 1 and 2 we give a visual comparison of the target organ AD for the [¹⁷⁷Lu]Lu-1C1m-Fc 1 DOTA and 3 DOTA respectively. This graphical representation gives

Table 3 Mice-to-human extrapolation for [⁶⁴Cu]Cu-1C1m-Fc 3 DOTA

[⁶⁴ Cu]Cu-1C1m-Fc 3 DOTA	TIAC (MBq.h/MBq)							
	M1		M2		M3		M4	
	M	F	M	F	M	F	M	F
Left colon	0.091	0.090	0.055	0.067	0.073	0.072	0.048	0.058
Small intestine	0.434	0.434	0.181	0.194	0.296	0.296	0.124	0.132
Stomach cont	0.096	0.096	0.084	0.094	0.077	0.077	0.067	0.075
Right colon	0.122	0.122	0.073	0.090	0.098	0.098	0.064	0.079
Rectum	0.059	0.060	0.035	0.044	0.047	0.048	0.031	0.039
Heart cont	0.513	0.508	0.146	0.128	2.645	2.645	0.754	0.665
Heart wall	0.187	0.187	0.151	0.139	0.175	0.175	0.141	0.130
Kidneys	0.585	0.585	0.165	0.178	0.645	0.645	0.182	0.196
Liver	2.689	2.689	1.164	1.101	2.429	2.429	1.051	0.995
Lungs	0.338	0.338	0.684	0.658	0.415	0.415	0.840	0.809
Ovaries		0.056		0.005		0.050		0.005
Red marrow	1.176	1.236	1.176	1.236	1.853	1.947	1.853	1.947
Spleen	0.194	0.194	0.087	0.092	0.209	0.209	0.093	0.098
Uterus		0.088		0.024		0.176		0.047
Total body	13.7	13.7	13.7	13.7	13.7	13.7	13.7	13.7
Rest of body	7.3	7.1	9.7	9.7	4.8	4.5	8.5	8.5

[⁶⁴Cu]Cu-1C1m-Fc 3 DOTA mice-to-human extrapolation of average source organ TIACs was obtained with the four considered dosimetry methods (M1-M4) for both the adult male (M) and female (F) human subjects

Table 4 AD to selected target organs for the [¹⁷⁷Lu]Lu-1C1m-Fc 1 DOTA and 3 DOTA

Target organ	[¹⁷⁷ Lu]Lu-1C1m-Fc (average) Absorbed dose (Gy/GBq)							
	M1		M2		M3		M4	
	1 DOTA	3 DOTA	1 DOTA	3 DOTA	1 DOTA	3 DOTA	1 DOTA	3 DOTA
Heart wall	0.37	0.23	0.36	0.15	0.89	0.58	0.59	0.35
Kidneys	1.09	0.66	0.30	0.19	1.48	1.28	0.41	0.34
Liver	1.30	1.79	0.51	0.68	1.27	1.79	0.50	0.70
Lungs	0.11	0.08	0.19	0.16	0.22	0.17	0.41	0.35
Ovaries	3.63	1.88	0.30	0.11	4.63	3.47	0.40	0.11
Red marrow	0.19	0.19	0.35	0.21	0.21	0.37	0.43	0.39
Spleen	0.72	0.73	0.30	0.35	1.35	0.74	0.39	0.35
Uterus	3.13	1.88	0.69	0.64	3.13	0.64	0.73	0.11
Total body	0.15	0.14	0.15	0.14	0.15	0.14	0.15	0.14
E (Sv/GBq)	0.27	0.26	0.18	0.18	0.34	0.36	0.22	0.22

The table reports average AD and the effective dose for the gender averaged human adult model obtained with the OLINDA/EXM 2.1 software for each tested dosimetry methods (M1-M4), for the [¹⁷⁷Lu]Lu-1C1m-Fc 1 DOTA and 3 DOTA

Table 5 ^{64}Cu AD to selected target organs and comparison with previously published data

Target organ	^{64}Cu Cu-1C1m-Fc 3DOTA (average) AD (mGy/MBq)				AD (mGy/MBq)	
	M1	M2	M3	M4	^{64}Cu Cu-DOTA-Trastuzumab [34]	^{89}Zr Zr-cmAb U36 [35]
Heart Wall	0.11	0.06	0.33	0.12	0.16	
Kidneys	0.17	0.06	0.19	0.06	0.09	1
Liver	0.16	0.07	0.15	0.06	0.12	1.3
Lungs	0.04	0.06	0.05	0.07		0.79
Ovaries	0.38	0.04	0.34	0.04		
Red Marrow	0.06	0.06	0.08	0.09	0.04	0.08
Spleen	0.12	0.06	0.13	0.06	0.10	0.72
Uterus	0.10	0.03	0.18	0.06		
E (mSv/MBq)	0.05	0.04	0.05	0.04	0.03	0.6

The table reports average AD and the effective dose for the gender averaged human adult model obtained with the OLINDA/EXM 2.1 software for each tested dosimetry methods (M1-M4). Original data for the ^{64}Cu Cu-1C1m-Fc 3DOTA are compared with previously published dosimetry from the ^{64}Cu Cu-DOTA-Trastuzumab [34] and the ^{89}Zr Zr-cmAb U36 [35] respectively

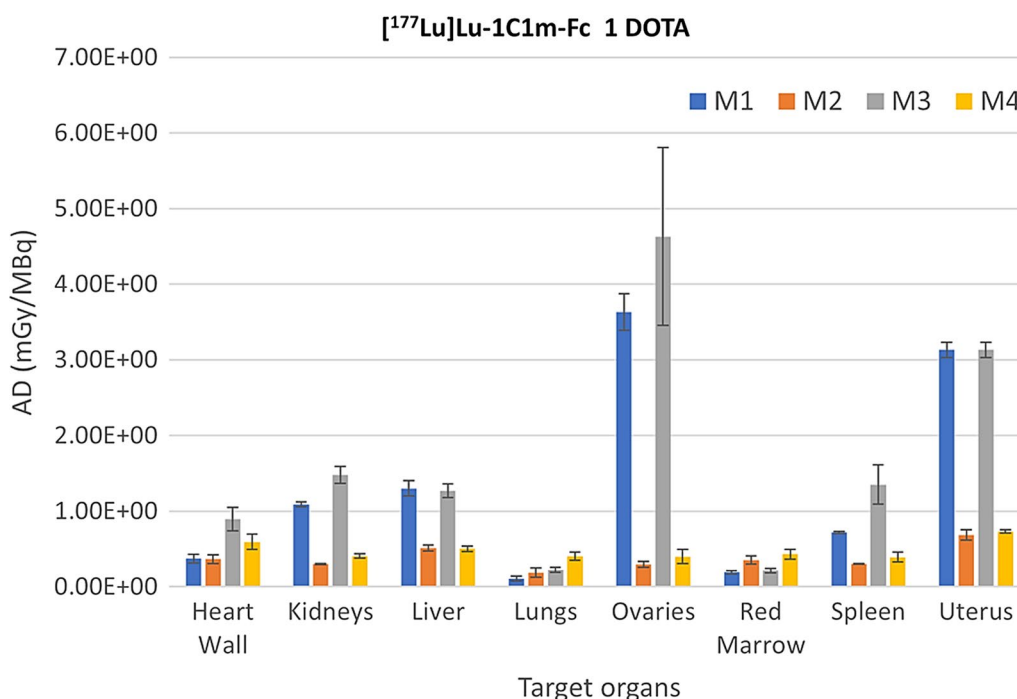


Fig. 1 AD in target organs for the ^{177}Lu Lu-1C1m-Fc 1DOTA. The figure shows the average, upper and lower AD in target organs as a function of the dosimetry extrapolation method used. Bars indicated upper/lower AD

the average AD with the upper/lower levels expressed by error bars.

The full data concerning AD in target organs for the male, female and gender averaged adult human subject including average, upper and lower values are reported in the Additional file 1: Tables S4, S5 and S6.

In Table 6 we reported the values of maximal administered activity compliant with the organ-specific AD safety limits reported in the materials and methods in prevision of a therapeutic use of the ^{177}Lu radiolabeled compounds.

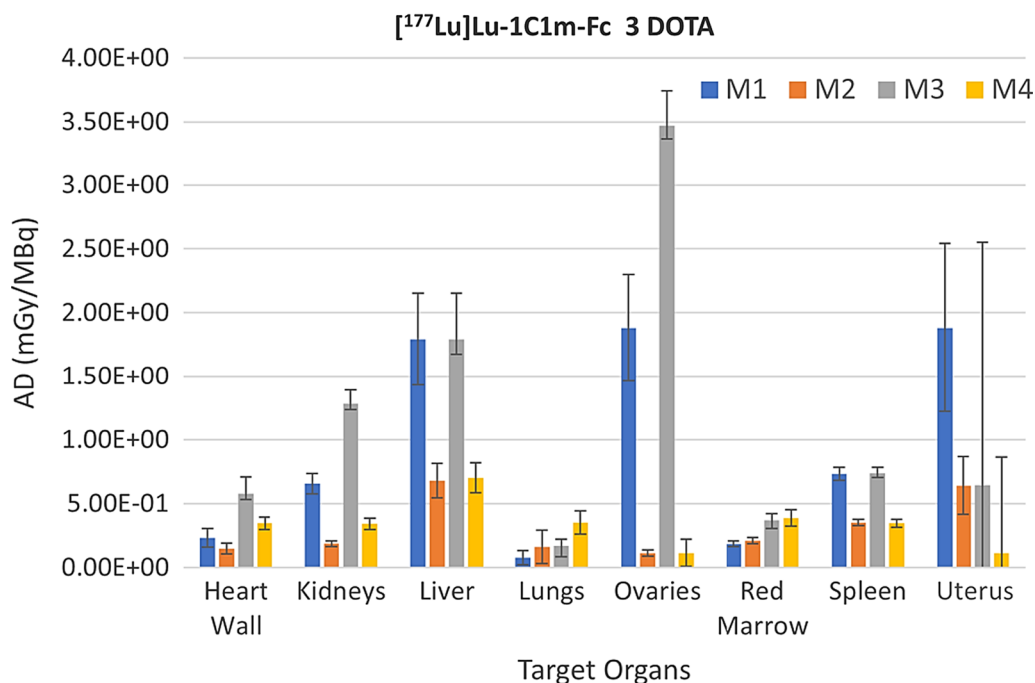


Fig. 2 AD in target organs for the ¹⁷⁷LuLu-1C1m-Fc 3DOTA. The figure shows average, upper and lower AD in target organs as a function of the dosimetry extrapolation method used. Bars indicated upper/lower AD

Table 6 Cumulated therapeutic activity to reach AD safety and efficacy levels

Target Organ (AD limit) [36]	Cumulated administered activity (GBq) to reach AD safety limit or AD efficacy threshold (in tumor)							
	M1		M2		M3		M4	
	1 DOTA	3 DOTA	1 DOTA	3 DOTA	1 DOTA	3 DOTA	1 DOTA	3 DOTA
Heart wall (30 Gy) [27]	80.4	129.3	82.4	204.1	33.6	51.8	50.7	87.0
Kidneys (30 Gy) [29]	27.5	45.8	100.3	161.3	20.3	23.4	74.1	88.0
Liver (40 Gy) [28]	30.8	22.3	78.3	58.7	31.5	22.3	79.8	57.0
Lungs (20 Gy) [27]	186.9	255.4	107.5	125.0	90.1	116.3	49.4	56.8
Red Marrow (2 Gy) [31]	10.5	10.8	5.7	9.6	9.4	5.4	4.7	5.2
Uterus (16 Gy) [30]	5.1	8.5	23.4	25.0	5.1	24.9	21.9	140.4
Total Body (4 Gy) [32]	25.5	28.8	25.5	28.8	25.5	28.8	25.5	28.8
Tumor STS (60 Gy) [33]	32.7	41.1						

The table reports the cumulated therapeutic administered activity required to reach limiting-organ AD safety limits and the efficacy AD thresholds of 60 Gy in STS for the ¹⁷⁷LuLu-1C1m-Fc 1 DOTA and 3 DOTA as a function of the mice-to-human dosimetry extrapolation method (M1-M4)

Discussion

We have presented and compared the mice-to-human dosimetry extrapolation of ¹⁷⁷Lu and ⁶⁴Cu radiolabeled TEM-1 obtained with four reference methods. For the three considered radiolabeled TEM-1 compounds we reported important variation of AD to target organs as a function of the considered dose-extrapolation method. This aspect was previously discussed in Cicone et al. [19].

Furthermore, insufficient information is presently available in the literature to determine which animal-to-human dosimetry extrapolation method is the more appropriate for a specific type of radiolabeled molecule. Most of the publications reporting animal-to-human dosimetry extrapolations used only one method, typically M1 or M2.

As indicated in Figs. 1 and 2, we found that the application of M1 and M3, which did not consider organ mass

scaling across species, resulted in significantly higher AD as compared to M2 and M4 in most considered target organs. This difference is more prominent in the female reproductive organs such as the uterus and the ovaries, for which AD obtained with M1 and M3 overestimate the AD obtained with M2 and M4 by a factor ranging from 4 to 10.

In particular, M4 takes into account two important factors of the inter-specie variability, such as the different metabolic rates, and the different relative organ masses compared to the individual whole body mass. Nevertheless, there is still poor scientific background to establish which of the tested methods for animal-to-human absorbed dose extrapolation would provide the better prediction. In most published literature, dosimetry extrapolation from pre-clinic setup to humans rely on the application of a single method and no systematic comparison with the in-human dosimetry is reported. Hence, based on the present knowledge we cannot argue for the superiority of one of the four tested methods. Future animal-to-human dosimetry comparison would hopefully provide more insight on this direction.

We observed that for many source organs TIACs (and hence AD) obtained by application of M2 and M4 presented similar values. The same is true for TIACs (and hence AD) obtained with M1 and M3. This is particularly true for organs such as the liver, that have a relatively large biological half life comparable to the physical half life (for instance: 137 and ~160 h respectively for the case of Lu-177 TEM-1 1DOTA) and consequently the contribution of the metabolic correction was relatively small. Larger differences between M2 and M4 have been reported for instance for the cardiac wall in reason of the larger difference between the biological and physical half life (37 and 160 h respectively for the cas of the Lu-177 TEM-1 1DOTA).

We also observed, methods M2 and M4 produced systematically higher values of TIAC (and hence AD) than M1 and M3. This resulted from the important impact of the application relative organ mass rescaling correction for the mice-to-human case on study.

Considering a possible future therapeutic use of the ^{177}Lu TEM-1 compounds, the AD estimates for target organs obtained with the different methods translate into different viable therapeutic cumulated activity administration levels that respect the safety limits in potentially critical organs (see Table 6).

From the results obtained in mice experiments, the ^{177}Lu Lu-1C1m-Fc conjugated with 1 DOTA presented the most favourable tumour-to-liver AD ratio of 1.4 [12]. Hence, we considered this form as an interesting candidate for a possible in-human therapeutic translation for the treatment of STS patients. Accessing a solid tumor

with a radiolabeled immuno-agent typically involves a long circulating half-life of the compound hence resulting in an important normal organ irradiation with a consequent, increased, haematological impact. This contrasts significantly with small peptides that are characterized by a rapid clearance and shorter tumour retention [16]. According to the obtained dose extrapolations for the human subject, the main constraint for the cumulated therapeutic administered activity of ^{177}Lu Lu-1C1m-Fc (1 DOTA) is determined by the safety dose limit of 2 Gy applied to the red-marrow. A single application of 5–10 GBq of this radiopharmaceutical would be sufficient to reach this safety limit. For the total body exposure, we retained a maximum acceptable dose of 4 Gy as indicated from the ^{131}I -I-MIBG treatment for neuroblastoma in pediatrics [32], where the 4 Gy safety limit was assumed as a surrogate estimation of the red-marrow AD exposure.

In our analysis we referred to organ AD safety limits from specific literature reports. However, it is reasonable to assume that, in the absence of a solid evidence-based background, such values may continue to evolve with the emergence of new findings. This is particularly relevant in the domain of radiopharmaceutical therapies where, unlike for EBRT, a diversity of both targeting molecules and radioisotopes must be considered [37].

In our dosimetry extrapolations this level of AD for the total body is reached with 25 GBq of total cumulated therapeutic activity. Considering a target AD of 60 Gy in the tumoral volume (values assumed from EBRT for the response of STS [33]), the required therapeutic activity is about 30 GBq, a value approaching the safety limits in other important organs (other than the red-marrow) such as the liver and the kidneys. Considering the results obtained so far, and a 30 GBq therapeutic activity administration to achieve 60 Gy to the STS, this would require a patient specific dosimetric optimization of the treatment plan.

To avoid toxicity due to the myelosuppression-related toxicity and to allow escalation of the therapeutic activity administration to myeloablative levels, a number of strategies have been tested such as autologous marrow reinfusion or injection of granulocyte-macrophage colony-stimulating factor [38]. In the context of radioimmunotherapy with ^{131}I , Press et al. [39] obtained a recovery of the number of neutrophils superior to 500/mm³ for a median (\pm SD) of 22 ± 9 days after marrow infusion, whereas platelet recovery was more variable, occurring at a median of 20 ± 27 days.

Moreover, fractionated therapeutic administration can be envisaged to decrease the haematological toxicity to acceptable levels [40]. Since 1C1m-Fc is a fully human fusion protein antibody, we expect that it may be

administered in repeated fractionated doses with a low immunogenicity risk and good predicted tolerance.

Special consideration should also be given to patient selection, in particular regarding any history of high dose chemotherapy which may increase the risk of developing bone marrow toxicity [41].

To explore the feasibility of a therapeutic approach based on the use of the [^{177}Lu]Lu-1C1m-Fc in treating STS, further investigations in larger size mammals such as dogs and/or pigs could provide complementary useful information. Such animal models expressing TEM-1 positive STS will enable a more robust tumour-to-normal organ and red marrow dosimetry evaluation. In contrast to our previous studies in mice, in which red-marrow dosimetry was performed based on blood data only, in larger mammals the red marrow dosimetry could be improved by PET and SPECT imaging assessment that would complement and improve the estimation based on the blood sample collection. Furthermore, we stress the fact that the level of toxicity in many organs such as the liver, the kidneys and the red-marrow itself are not sufficiently characterized for the systemic administration of ^{177}Lu labeled radiotherapeutics. This aspect is of key relevance and could be addressed in future 'bridging' studies in eg. dogs or pigs before progressing to in-human therapeutic applications. Dose-toxicity thresholds for ^{177}Lu radioligands (^{177}Lu -DOTA and ^{177}Lu -PSMA) have not yet been defined [42–44]. Even the commonly accepted 2 Gy safety limits for the red marrow derives from historic data in ^{131}I therapy [31], more recent dosimetric results increase this level to 3 Gy [45]. Previous experience with therapeutic administration of ^{90}Y -Ibritumomab-Tiuxetan do not report correlations between bone marrow AD and hemato-toxicity for bone marrow AD of 2 Gy. Rather, the hemato-toxicity correlated with the elapsed time from the last chemotherapy [41]. Moreover the AD threshold level for tumour response using ^{177}Lu antibodies in STS is an unresolved issue that could be investigated with the escalation of the administered activity in such animal models.

In view of developing a full theranostic approach, we reported the mice-to-human extrapolation of the AD and E for the [^{64}Cu]Cu-1C1m-Fc as a PET companion tracer of the [^{177}Lu]Lu-1C1m-Fc. We compared AD estimations obtained from the four extrapolation methods with in-human dosimetric results reported in the literature for radiolabeled antibodies, namely: [^{64}Cu]Cu-DOTA-Trastuzumab [34] and [^{89}Zr]Zr-cmAb U36 [35].

[^{64}Cu]Cu-DOTA-Trastuzumab was used in a clinical trial for PET/CT functional imaging of human epidermal growth factor receptor 2-positive metastatic breast cancer. Such a radiolabeled antibody presented similar effective dose and AD levels in targeted organs to the

extrapolated human ADs reported by ourselves for the [^{64}Cu]Cu-1C1m-Fc. The use of a ^{64}Cu PET immuno-tracer is ideal for the short-term characterization of the uptake of the radiolabeled antibody particle in lesions within the two days after the diagnostic administration [34], thus providing key information for patient selection. However, because of the relatively short physical half-life (12.7 h), ^{64}Cu PET immuno-tracers are not suited for pre-therapeutic dosimetry planning. [^{89}Zr]Zr-cmAb U36 presented higher effective dose and higher AD level than our radiolabeled compound (Table 5). The use of ^{89}Zr -radiolabeled immunotracers have shown promising results enabling the characterization of the biokinetics in tissues for a sufficiently long period of time (typically up to one week) [35]. Nevertheless, the relatively long half-life involves a less favorable dosimetry, limited availability of radionuclide, and patient convenience issues, since patients are required to return about 5 days after tracer administration [46].

Conclusions

Dose estimation based on animal data is a mandatory requirement, providing important insights and guidance for predicting safety and efficacy of any radiolabeled compound prior to its diagnostic and/or therapeutic in-human translation. Different methods for animal-to-human dosimetry extrapolations have been reported in the literature but no consensus presently exists on the appropriate approach to apply for any specific radiolabeled compound. For the theranostic couple $^{64}\text{Cu}/^{177}\text{Lu}$ 1C1m-Fc anti TEM-1, we show an important variability in mice-to-human AD extrapolations depending on the method used. Furthermore, in considering a potential therapeutic application of [^{177}Lu]Lu-1C1m-Fc, further dosimetry analysis supported by quantitative imaging investigations performed in a large mammal species bearing STS would prove highly informative.

Supplementary Information

The online version contains supplementary material available at <https://doi.org/10.1186/s13550-023-01010-4>.

Additional file 1: Table S1 TIAC for the [^{177}Lu]Lu-1C1m-Fc 1 DOTA. **Table S2** TIAC for the [^{177}Lu]Lu-1C1m-Fc 3 DOTA. **Table S3** TIAC for the [^{64}Cu]Cu-1C1m-Fc 3 DOTA. **Table S4** Target organ AD for the [^{177}Lu]Lu-1C1m-Fc 1 DOTA. **Table S5** Target organ AD for the [^{177}Lu]Lu-1C1m-Fc 3 DOTA. **Table S6** Target organ AD for the [^{64}Cu]Cu-1C1m-Fc 3 DOTA.

Acknowledgements

We thank the Radioactivity platform (SFR Santé), for expert technical assistance. We thank the cyclotron Arronax for supply of copper-64. We thank Prof George Coukos (Ludwig Institute for Cancer Research and Department of Oncology, Lausanne University Hospital and University of Lausanne, CH-1011 Lausanne, Switzerland) for supporting this research work and participating to funding acquisition.

Author contributions

Study design: JAD, SG. Generation of dosimetry data: SG. Conduction of animal experiments: JAD. Data analysis and critical evaluation of the results: JOP, SMD, NC, AFC, NS, MC. Manuscript writing: JAD, SG. All authors read and approved the final manuscript.

Funding

Open access funding provided by University of Lausanne. This research was funded with the help of the Alfred and Annemarie von Sikk Grant (Zurich, Switzerland) and the Department of Nuclear Medicine and Molecular Imaging, Lausanne University Hospital (Lausanne, Switzerland). This research was also funded in part by grants from the French National Agency for Research, called "Investissements d'Avenir" IRON LabEx n° ANR-11-LABX-0018-01, IGO LabEx n° ANR-11-LABX-0016-01, Siric ILIAD, DHU Oncogreff, ArronaxPlus Equipex n° ANR-11-EQPX-0004 and NEXt n° ANR-16-IDEX-0007.

Availability of data and materials

The datasets used and/or analyzed during the current study are available from the corresponding author on reasonable request.

Declarations

Ethics approval and consent to participate

All animal experiments were conducted in compliance either with the ARRIVE guidelines and according to the Swiss regulations (can-tonal authorization VD-2993) and the guidelines of the Lausanne University Hospital, or with the French regulations and approved by the local animal ethics committee (APAFIS#6145). In this case, animals were housed under specific pathogen-free conditions in the UTE animal facility (SFR François Bonamy, IRS-UN, University of Nantes, license number: C-44-278).

Consent for publication

Not applicable.

Competing interests

The authors declare that they have no competing interests.

Received: 24 April 2023 Accepted: 6 June 2023

Published online: 14 June 2023

References

- Teicher BA. CD248: a therapeutic target in cancer and fibrotic diseases. *Oncotarget*. 2019;10(9):993–1009.
- MacFadyen J, Savage K, Wienke D, Isacke CM. Endosialin is expressed on stromal fibroblasts and CNS pericytes in mouse embryos and is down-regulated during development. *Gene Expr Patterns*. 2007;7(3):363–9.
- Bagley RG, Honma N, Weber W, Boutin P, Rouleau C, Shankara S, et al. Endosialin/TEM 1/CD248 is a pericyte marker of embryonic and tumor neovascularization. *Microvasc Res*. 2008;76(3):180–8.
- Davies G, Cunnick GH, Mansel RE, Mason MD, Jiang WG. Levels of expression of endothelial markers specific to tumour-associated endothelial cells and their correlation with prognosis in patients with breast cancer. *Clin Exp Metastasis*. 2004;21(1):31–7.
- O'Shannessy DJ, Somers EB, Chandrasekaran LK, Nicolaidis NC, Bordeaux J, Gustavson MD. Influence of tumor microenvironment on prognosis in colorectal cancer: tissue architecture-dependent signature of endosialin (TEM-1) and associated proteins. *Oncotarget*. 2014;5(12):3983–95.
- Kontsekova S, Polcova K, Takacova M, Pastorekova S. Endosialin: molecular and functional links to tumor angiogenesis. *Neoplasma*. 2016;63(2):183–92.
- Valdez Y, Maia M, Conway EM. CD248: reviewing its role in health and disease. *Curr Drug Targets*. 2012;13(3):432–9.
- Guo Y, Hu J, Wang Y, Peng X, Min J, Wang J, et al. Tumour endothelial marker 1/endosialin-mediated targeting of human sarcoma. *Eur J Cancer*. 2018;90:111–21.
- Thway K, Robertson D, Jones RL, Selfe J, Shipley J, Fisher C, et al. Endosialin expression in soft tissue sarcoma as a potential marker of undifferentiated mesenchymal cells. *Br J Cancer*. 2016;115(4):473–9.
- Edge SB, Compton CC. The American Joint Committee on Cancer: the 7th edition of the AJCC cancer staging manual and the future of TNM. *Ann Surg Oncol*. 2010;17(6):1471–4.
- Herrmann K, Schwaiger M, Lewis JS, Solomon SB, McNeil BJ, Baumann M, et al. Radiotheranostics: a roadmap for future development. *Lancet Oncol*. 2020;21(3):e146–56.
- Delage JA, Gnesin S, Prior JO, Barbet J, Le Saec P, Marionneau-Lambot S, et al. Copper-64-Labeled 1C1m-Fc, a new tool for TEM-1 PET imaging and prediction of Lutetium-177-Labeled 1C1m-Fc therapy efficacy and safety. *Cancers (Basel)*. 2021;13(23):5936.
- Delage JA, Faivre-Chauvet A, Fierle JK, Gnesin S, Schaefer N, Coukos G, et al. (177)Lu radiolabeling and preclinical theranostic study of 1C1m-Fc: an anti-TEM-1 scFv-Fc fusion protein in soft tissue sarcoma. *EJNMMI Res*. 2020;10(1):98.
- Delage JA, Faivre-Chauvet A, Barbet J, Fierle JK, Schaefer N, Coukos G, et al. Impact of DOTA conjugation on pharmacokinetics and immunoreactivity of [(177)Lu]Lu-1C1m-Fc, an Anti-TEM-1 fusion protein antibody in a TEM-1 positive tumor mouse model. *Pharmaceutics*. 2021;13(1):96.
- Karimian A, Ji NT, Song H, Sgouros G. Mathematical modeling of preclinical alpha-emitter radiopharmaceutical therapy. *Cancer Res*. 2020;80(4):868–76.
- Sgouros G, Bodei L, McDevitt MR, Nedrow JR. Radiopharmaceutical therapy in cancer: clinical advances and challenges. *Nat Rev Drug Discov*. 2020;19(9):589–608.
- Kranz M, Sattler B, Tiepolt S, Wilke S, Deuther-Conrad W, Donat CK, et al. Radiation dosimetry of the alpha(4)beta(2) nicotinic receptor ligand (+)-[(18)F]flubatine, comparing preclinical PET/MRI and PET/CT to first-in-human PET/CT results. *EJNMMI Phys*. 2016;3(1):25.
- Korde A, Mikolajczak R, Kolenc P, Bouziotis P, Westin H, Lauritzen M, et al. Practical considerations for navigating the regulatory landscape of non-clinical studies for clinical translation of radiopharmaceuticals. *EJNMMI Radiopharm Chem*. 2022;7(1):18.
- Cicone F, Viertl D, Denoel T, Stabin MG, Prior JO, Gnesin S. Comparison of absorbed dose extrapolation methods for mouse-to-human translation of radiolabelled macromolecules. *EJNMMI Res*. 2022;12(1):21.
- Fierle JK, Abram-Saliba J, Brioschi M, deTiani M, Coukos G, Dunn SM. Integrating SpyCatcher/SpyTag covalent fusion technology into phage display workflows for rapid antibody discovery. *Sci Rep*. 2019;9(1):12815.
- Cicone F, Denoel T, Gnesin S, Riggi N, Irving M, Jakka G, et al. Preclinical Evaluation and Dosimetry of [(111)In]CHX-DTPA-scFv78-Fc Targeting Endosialin/Tumor Endothelial Marker 1 (TEM1). *Mol Imaging Biol*. 2020;22(4):979–91.
- Beykan S, Fani M, Jensen SB, Nicolas G, Wild D, Kaufmann J, et al. In vivo biokinetics of (177)Lu-OPS201 in mice and pigs as a model for predicting human dosimetry. *Contrast Media Mol Imaging*. 2019;2019:6438196.
- Sparks RA, B. Comparison of the effectiveness of some common animal data scaling techniques in estimating human radiation dose. In: Proceedings of sixth international radiopharmaceutical dosimetry symposium Oak Ridge, TN, USA; 1999
- Valentin J. Basic anatomical and physiological data for use in radiological protection reference values. *Ann ICRP*. 2002;32(3–4):1–277.
- Stabin MG, Siegel JA. RADAR dose estimate report: a compendium of radiopharmaceutical dose estimates based on OLINDA/EXM version 20. *J Nucl Med*. 2018;59(1):154–60.
- Valentin J. The 2007 recommendations of the international commission on radiological protection. *Ann ICRP*. 2007;37(2–4):1–133.
- Kong FM, Ritter T, Quint DJ, Senan S, Gaspar LE, Komaki RU, et al. Consideration of dose limits for organs at risk of thoracic radiotherapy: atlas for lung, proximal bronchial tree, esophagus, spinal cord, ribs, and brachial plexus. *Int J Radiat Oncol*. 2011;81(5):1442–57.
- Levillain H, Bagni O, Deroose CM, Dieudonne A, Gnesin S, Grosser OS, et al. International recommendations for personalised selective internal radiation therapy of primary and metastatic liver diseases with yttrium-90 resin microspheres. *Eur J Nucl Med Mol Imaging*. 2021;48(5):1570–84.
- Sjogreen Gleisner K, Chouin N, Gabina PM, Cicone F, Gnesin S, Stokke C, et al. EANM dosimetry committee recommendations for dosimetry of 177Lu-labelled somatostatin-receptor- and PSMA-targeting ligands. *Eur J Nucl Med Mol Imaging*. 2022;49(6):1778–809.

30. Lohynska R, Jirkovska M, Novakova-Jiresova A, Mazana E, Vambersky K, Veselsky T, et al. Radiotherapy dose limit for uterus fertility sparing in curative chemoradiotherapy for rectal cancer. *Biomed Pap Med Fac Univ Palacky Olomouc Czech Repub.* 2021;165(1):99–101.
31. Benua RS, Cicale NR, Sonenberg M, Rawson RW. The relation of radioiodine dosimetry to results and complications in the treatment of metastatic thyroid cancer. *Am J Roentgenol Radium Ther Nucl Med.* 1962;87:171–82.
32. Gaze MN, Chang YC, Flux GD, Mairs RJ, Saran FH, Meller ST. Feasibility of dosimetry-based high-dose ¹³¹I-meta-iodobenzylguanidine with topotecan as a radiosensitizer in children with metastatic neuroblastoma. *Cancer Biother Radiopharm.* 2005;20(2):195–9.
33. Rosenberg SA, Tepper J, Glatstein E, Costa J, Baker A, Brennan M, et al. The treatment of soft-tissue sarcomas of the extremities—prospective randomized evaluations of (1) limb-sparing surgery plus radiation-therapy compared with amputation and (2) the role of adjuvant chemotherapy. *Ann Surg.* 1982;196(3):305–15.
34. Mortimer JE, Bading JR, Colcher DM, Conti PS, Frankel PH, Carroll MI, et al. Functional imaging of human epidermal growth factor receptor 2-positive metastatic breast cancer using (64)Cu-DOTA-trastuzumab PET. *J Nucl Med.* 2014;55(1):23–9.
35. Borjesson PK, Jauw YW, de Bree R, Roos JC, Castelijns JA, Leemans CR, et al. Radiation dosimetry of ⁸⁹Zr-labeled chimeric monoclonal antibody U36 as used for immuno-PET in head and neck cancer patients. *J Nucl Med.* 2009;50(11):1828–36.
36. Emami B, Lyman J, Brown A, Coia L, Goitein M, Munzenrider JE, et al. Tolerance of normal tissue to therapeutic irradiation. *Int J Radiat Oncol Biol Phys.* 1991;21(1):109–22.
37. Wahl RL, Sgouros G, Irvani A, Jacene H, Pryma D, Saboury B, et al. Normal-tissue tolerance to radiopharmaceutical therapies, the knowns and the unknowns. *J Nucl Med.* 2021;62(Suppl 3):235–355.
38. Sharkey RM, Brenner A, Burton J, Hajjar G, Toder SP, Alavi A, et al. Radioimmunotherapy of non-Hodgkin's lymphoma with ⁹⁰Y-DOTA humanized anti-CD22 IgG (90Y-Epratuzumab): do tumor targeting and dosimetry predict therapeutic response? *J Nucl Med.* 2003;44(12):2000–18.
39. Press OW, Eary JF, Appelbaum FR, Martin PJ, Badger CC, Nelp WB, et al. Radiolabeled-antibody therapy of B-cell lymphoma with autologous bone marrow support. *N Engl J Med.* 1993;329(17):1219–24.
40. Linden O, Hindorf C, Cavallin-Stahl E, Wegener WA, Goldenberg DM, Horne H, et al. Dose-fractionated radioimmunotherapy in non-Hodgkin's lymphoma using DOTA-conjugated, ⁹⁰Y-radiolabeled, humanized anti-CD22 monoclonal antibody, epratuzumab. *Clin Cancer Res.* 2005;11(14):5215–22.
41. Baechler S, Hobbs RF, Jacene HA, Bochud FO, Wahl RL, Sgouros G. Predicting hematologic toxicity in patients undergoing radioimmunotherapy with ⁹⁰Y-ibritumomab tiuxetan or ¹³¹I-tositumomab. *J Nucl Med.* 2010;51(12):1878–84.
42. Cremonesi M, Ferrari ME, Bodei L, Chiesa C, Sarnelli A, Garibaldi C, et al. Correlation of dose with toxicity and tumour response to (90)Y- and (177)Lu-PRRT provides the basis for optimization through individualized treatment planning. *Eur J Nucl Med Mol Imaging.* 2018;45(13):2426–41.
43. Sundlov A, Sjogreen-Gleisner K. Peptide receptor radionuclide therapy—prospects for personalised treatment. *Clin Oncol (R Coll Radiol).* 2021;33(2):92–7.
44. Lassmann M, Hanscheid H, Chiesa C, Hindorf C, Flux G, Luster M, et al. EANM Dosimetry Committee series on standard operational procedures for pre-therapeutic dosimetry I: blood and bone marrow dosimetry in differentiated thyroid cancer therapy. *Eur J Nucl Med Mol Imaging.* 2008;35(7):1405–12.
45. Dorn R, Kopp J, Vogt H, Heidenreich P, Carroll RG, Gulec SA. Dosimetry-guided radioactive iodine treatment in patients with metastatic differentiated thyroid cancer: largest safe dose using a risk-adapted approach. *J Nucl Med.* 2003;44(3):451–6.
46. Carrasquillo JA, Morris PG, Humm JL, Smith-Jones PM, Beylertgil V, Akhurst T, et al. Copper-64 trastuzumab PET imaging: a reproducibility study. *Q J Nucl Med Mol Imaging.* 2019;63(2):191–8.

Publisher's Note

Springer Nature remains neutral with regard to jurisdictional claims in published maps and institutional affiliations.

Submit your manuscript to a SpringerOpen[®] journal and benefit from:

- Convenient online submission
- Rigorous peer review
- Open access: articles freely available online
- High visibility within the field
- Retaining the copyright to your article

Submit your next manuscript at ► [springeropen.com](https://www.springeropen.com)